nature reviews physics

https://doi.org/10.1038/s42254-025-00829-1

Review article

Check for updates

Nonlocal metamaterials and metasurfaces

Yi Chen [1,2] ✉, Romain Fleury [3], Pierre Seppecher[4], Gengkai Hu[5] & Martin Wegener [1,2] ✉

Abstract

The aim of rationally designed composites called metamaterials or metasurfaces is to achieve effective properties that go beyond those of their constituent parts. For periodic architectures, the design can draw on concepts from solid-state physics, such as crystal symmetries, reciprocal space, band structures and Floquet–Bloch eigenfunctions. Recently, nonlocality has emerged as a design paradigm, enabling both static and dynamic properties that are unattainable with a local design. In principle, all material properties described by linear response functions can be nonlocal, but for ordinary solids, local descriptions are mostly good approximations, leaving nonlocal effects as corrections. However, metamaterials and metasurfaces can be designed to go far beyond local behaviour. This Review covers these anomalous behaviours in elasticity, acoustics, electromagnetism, optics and diffusion. In the dynamic regime, nonlocal interactions enable versatile band structure and refraction engineering. In the static regime, they result in large decay lengths of 'frozen' evanescent Bloch modes, leading to strong size effects. For zero modes, the decay length diverges.

Sections

Introduction

Nonlocal metamaterials

Nonlocal metasurfaces

Outlook

[1]Institute of Nanotechnology, Karlsruhe Institute of Technology (KIT), Karlsruhe, Germany. [2]Institute of Applied Physics, Karlsruhe Institute of Technology (KIT), Karlsruhe, Germany. [3]Laboratory of Wave Engineering, École Polytechnique Fédéral de Lausanne (EPFL), Lausanne, Switzerland. [4]Institut de Mathematiques de Toulon, Universite de Toulon, Toulon, France. [5]School of Aerospace Engineering, Beijing Institute of Technology (BIT), Beijing, China. ✉e-mail: yi.chen@partner.kit.edu; martin.wegener@kit.edu

Key points

- Metamaterials are rationally designed composites with effective properties that go beyond their constituents. Following this definition, metamaterials include photonic and phononic crystals.
- (Meta)material response functions can be phenomenological or result from a theoretical homogenization procedure. For nonlocal materials, the response function at a given location depends not only on the field at that location but also on the field at other locations.
- We review nonlocal metamaterials for diverse physical fields according to three unified physical mechanisms to incorporate nonlocality, that is, beyond-nearest-neighbour interactions, chirality and delocalized zero modes.
- The nonlocal mechanisms mentioned earlier can lead to interesting wave properties, such as roton-like dispersion, topological insulators with large winding number, chiral eigenmodes and frequency splitting and anomalous dispersion cones.
- Nonlocality also induces static properties with anomalously large characteristic lengths, connected to frozen evanescent modes (evanescent Bloch modes at zero frequency) emerging from local minima on dispersion relations.
- Time dependence is introduced as a separate and emerging method to achieve nonlocal responses in metamaterials, that is, the time-reflection coefficient and time-refraction coefficient become spatially dispersive or wavenumber-dependent.
- Nonlocal metasurfaces often use leaky-wave modes or physical coupling to build nonlocal interactions in metasurfaces, enabling high frequency selectivity or performing spatial derivatives on incident wave fields.

Introduction

Natural materials composed of atoms and artificial materials — metamaterials — composed of tailored building blocks or 'meta-atoms'[1] form the basis for any kind of device and system in electronics, mechanics, acoustics and photonics. In the process of designing devices such as computer chips, mechanical support structures, acoustic insulation or photonic circuitry, one needs specific macroscopic descriptions of the (effective) response functions of the involved (meta)materials. These response functions can be phenomenological or can arise from a theoretical homogenization procedure and include the electric conductivity, the Young's modulus, the compressibility or the optical permittivity in their special local form[2–4]. One example of a local response function is the microscopic form of the static version of Ohm's law $j = \sigma E$ (ref. 5). The current density $j = j(x)$ at position x is proportional to the electric field $E = E(x)$ at the same position and the conductivity $\sigma \neq \sigma(x)$ is constant for a homogeneous material. Other examples include Hooke's law of elasticity and its generalizations in continuum mechanics[2,6], Fick's first law of diffusion[4], Fourier's law of heat conduction[3] as well as magnetic and electric susceptibilities in electromagnetism and optics[5]. Locality has immediate consequences. For the macroscopic form of Ohm's law, the resistance $R \propto L$ of a wire is simply proportional to the length of the wire L, because one can decompose the wire into a set of resistors in series, each of which follows a local version of Ohm's law. This simple behaviour forms the basis for resistive touch screens.

Nonlocal responses cover a much broader class of behaviours[5], containing local responses as special cases. For example, in one dimension, the nonlocal form of Ohm's law is defined by

$$j(x) = \int_{-\infty}^{\infty} \sigma'(x - x')E(x')\mathrm{d}x'. \tag{1}$$

From equation (1), we see that the current density $j(x)$ at location x depends on the electric field $E(x')$ at many other locations $x' \neq x$ by a mathematical convolution with the nonlocal electric conductivity $\sigma'(x - x')$. For the special case of $\sigma'(x - x') = \sigma\ \delta(x - x')$, with δ being the Dirac Delta function, a local response is recovered. By Fourier transformation of the nonlocal form, we obtain

$$\tilde{j}(k) = \tilde{\sigma}(k)\tilde{E}(k) \tag{2}$$

via the convolution theorem[5]. Herein, the conductivity $\tilde{\sigma}(k)$ explicitly depends on the spatial frequency or wavenumber k. Such behaviour is often referred to as spatial dispersion[5], which is directly linked to nonlocality.

Let us consider the special case that we can expand the function $\tilde{\sigma}(k)$ in equation (2) in a Taylor series as $\tilde{\sigma}(k) = \sigma_0 + \xi_1 k^1 + \xi_2 k^2 + \xi_3 k^3 \ldots$, with coefficients ξ_1, ξ_2, ... Insert this expansion into equation (2) and Fourier transform back to real space with, for example, $k\tilde{E}(k) \to -\mathrm{i}\mathrm{d}E(x)/\mathrm{d}x$ (ref. 5), leads to the form

$$j(x) = \sigma_0 E(x) - \mathrm{i}\xi_1\frac{\mathrm{d}E}{\mathrm{d}x} - \xi_2\frac{\mathrm{d}^2E}{\mathrm{d}x^2} + \mathrm{i}\xi_3\frac{\mathrm{d}^3E}{\mathrm{d}x^3} - \xi_4\frac{\mathrm{d}^4E}{\mathrm{d}x^4} + \ldots. \tag{3}$$

We can also equivalently reformulate equation (3) to a set of coupled first-order equations by introducing auxiliary quantities $a_j(x)$ ($j = 1, 2\ldots$):

$$\begin{cases} j(x) = \sigma_0 E(x) - \mathrm{i}\xi_1 a_1(x) - \xi_2 a_2(x) + \ldots \\ a_1(x) = \dfrac{\mathrm{d}E(x)}{\mathrm{d}x} \\ a_2(x) = \dfrac{\mathrm{d}a_1(x)}{\mathrm{d}x} \\ \vdots \end{cases} \tag{4}$$

We see that we can express nonlocality mathematically in at least four different ways: in terms of a spatial convolution integral (equation (1)), as a wavenumber dependence (equation (2)), as higher-order spatial derivatives (equation (3)) or as a set of coupled first-order equations in equation (4). We will see below that all four ways generally lead to anomalous behaviour such as size effects and characteristic length scales.

For materials that exhibit chirality[7], which is defined by the lack of a centre of inversion, the absence of mirror planes and the absence of rotation-reflection symmetries, the odd-order and even-order terms can generally be non-zero. For achiral media, the odd-order terms are zero by crystal symmetry, $0 = \xi_1 = \xi_3 = \xi_5 = \ldots$.

It is generally demanding to derive the aforementioned phenomenological nonlocal descriptions from the microscopic Hamiltonian of a system. Nevertheless, it is instructive to discuss a simple example model that leads to nonlocal behaviour: in equation (5), we

consider a 1D tight-binding Hamiltonian H in matrix representation with local energies E_0 and wavefunctions $\varphi_n = \phi_0(x - \mathrm{na})$ with $n = -\infty, \ldots, -1, 0, +1, \ldots, +\infty$. These wavefunctions are localized at sites $x = x_n = \mathrm{na}$, in which a is the period or lattice constant. V_1 shall be the interaction energy between the immediate neighbours to the left (−) and the right (+), that is, the local interaction. V_N shall be the interaction energies with the $\pm N$th nearest neighbours (with $N = 2, 3, \ldots$), that is, the nonlocal interactions. From this Hamiltonian

$$H = \begin{pmatrix} \ddots & & & & & \iddots \\ & E_0 & V_1 & V_2 & V_3 & \\ & V_1 & E_0 & V_1 & V_2 & \\ & V_2 & V_1 & E_0 & V_1 & \\ & V_3 & V_2 & V_1 & E_0 & \\ \iddots & & & & & \ddots \end{pmatrix} \quad (5)$$

we obtain the (real-valued) eigenenergies $E = \hbar\omega$ of the Bloch wavefunctions versus wavenumber k

$$E(k) = E_0 + 2\sum_{N=1}^{\infty} V_N \cos(Nka). \quad (6)$$

From equation (6), it is immediately clear that this energy dispersion relation is an infinite Fourier series with Fourier coefficients $2V_N$, allowing to Fourier-synthesize any wanted behaviour for $E(k)$ within the first Brillouin zone $k \in [-\pi/a, +\pi/a]$, at least in principle. By contrast, without nonlocal interactions, that is, for $V_2 = V_3 = \ldots = 0$, we always get the simple cosine shape $E(k) = E_0 + 2V_1\cos(ka)$. The dispersion relation or band structure in equation (6) describes propagating Bloch waves with real-valued k as well as Bloch waves with complex-valued k, for which the wavelength at a given k is $\lambda = |2\pi/(\mathrm{Re}(k))|$ and the exponential decay length is given by $l = |1/\mathrm{Im}(k)|$. We refer to the latter as evanescent waves even if $\mathrm{Re}(k) \neq 0$. Examples of evanescent Bloch waves at finite frequencies are surface waves, which sometimes have a topological origin[8–11]. There also exist evanescent Bloch waves at zero frequency (the so-called frozen evanescent waves)[12]. Furthermore, there are non-Bloch solutions at finite frequencies and zero frequency[12,13].

We note in passing that the physics and the notion of nonlocal interactions become less clear if we use a larger or extended unit cell instead of the primitive cell or Wigner–Seitz cell[14]. In this case, nonlocal interactions turn into particular inner degrees of freedom within the extended unit cell. Of course, the nonlocal material properties discussed earlier do not depend on the choice of the unit cell – which is why we have defined nonlocality on the basis of the macroscopic material properties rather than on the basis of the microscopic structure of the (meta)material.

For atomic materials and crystals, the long-range Coulomb interaction between electrically charged particles introduces nonlocal interactions, but we cannot engineer the nonlocal coefficients $2V_{N>1}$ at will. Nature has done that. Nevertheless, nonlocal effects can be important in atomic materials[15]. The situation is different for nonlocal metamaterials. Here, quantum mechanics is usually not directly relevant. We can replace the quantum-mechanical wavefunction by a classical pressure field, a displacement field, an electric or a magnetic field. This aspect has been extensively discussed in a recent roadmap[16]. The interactions, analogous to the energies V_N in equation (5), can be designed and realized by periodically arranging pipes (acoustics), rods (elasticity), waveguides (optics and elasticity), cables (electromagnetism) or wires (Ohm's conduction) in real space. Mathematically, nonlocality cannot appear in strictly 1D microstructures[17]. One therefore needs 3D microstructures to avoid unwanted crossings of the connecting elements – even if one only targets a 1D periodic metamaterial architecture, as shown in Fig. 1a.

This Review is structured into nonlocal metamaterials and nonlocal metasurfaces. Both are always structures in 3D space and may be periodic along one, two or three directions. What is different is the spirit. For metamaterials, the aim is to tailor the behaviour of waves inside the metamaterial. One grasps that behaviour by band structures and Floquet–Bloch eigenfunctions. Under suitable conditions, approximate effective-medium descriptions in terms of equivalent continua may apply. We cover elasticity, acoustics, electromagnetic waves and electric conduction (a diffusion-type problem), but structure this part according to the mechanisms giving rise to nonlocality: beyond-nearest-neighbour interactions, chirality, delocalized zero modes and time dependencies. For metasurfaces, the aim is to engineer the direction, polarization and amplitude of waves outside the metasurface emerging by anomalous effective refraction or reflection from the metasurface, seen as a thin slab of material. Here, nonlocality means that the reflection or refraction at one position x of the interface not only depends on the metasurface properties at that positions but also on the properties at many other positions x' within the 2D metasurface. Nonlocal metasurfaces for optics and acoustics have recently been reviewed in detail[18–20]. Therefore, we do cover nonlocal metasurfaces, but emphasize recent progress with respect to refs. 18–20.

Nonlocal metamaterials

In Fig. 2, we depict several examples of nonlocal metamaterials, which are all based on the three mechanisms we will discuss in the following.

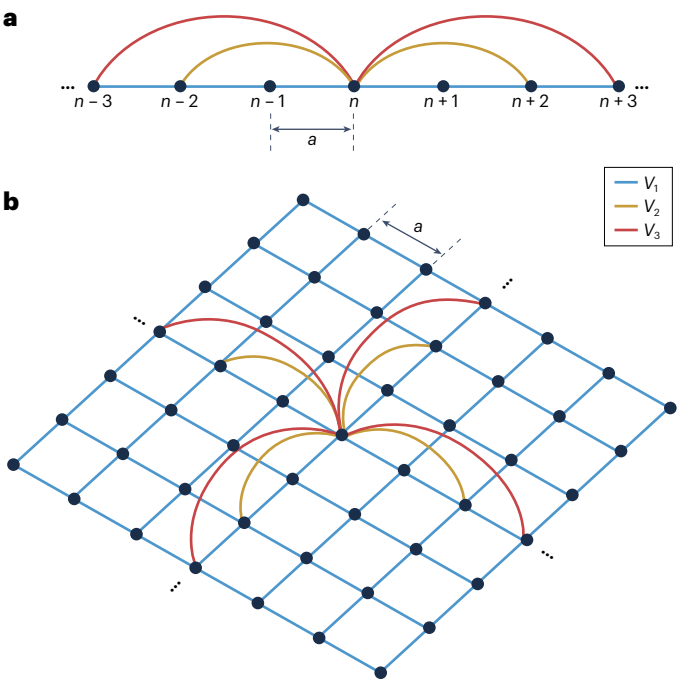

Fig. 1 | Illustration of nonlocal interactions in a tight-binding model. a, 1D system with period a and nonlocal interactions. V_1 represents local interactions between nearest-neighbour sites (for example, n and $n+1$), whereas V_2 and V_3 stand for nonlocal interactions between two sites separated by a distance of $2a$ and $3a$, respectively. For clarity, only four such nonlocal interactions are shown. **b**, Corresponding 2D nonlocal system.

The first and perhaps most straightforward way to introduce strong nonlocality following Fig. 1 is to couple metamaterial unit cells with their beyond-nearest-neighbours via physical components (Fig. 2a–e). This concept has been successfully realized for elastic waves[21–31], acoustic waves[32–35], radiofrequency electromagnetic waves[36,37] and electric conduction in metawires[38] (Fig. 2h). Alternatively, pronounced nonlocal interactions can be effectively achieved in metamaterials (Fig. 2f) by leveraging a special type of zero modes, called delocalized zero modes[39]. We will explain in detail the mechanism later. Furthermore, structures that are chiral (Fig. 2g) can exhibit unique nonlocal responses impossible to achieve with achiral metamaterials[40–42]. Here, chirality[7] means the absence of a centre of inversion, the absence of mirror planes and the absence of rotation–reflection symmetries of the metamaterial crystal. We discuss these three types of nonlocal mechanisms in the following three sections.

Beyond-nearest-neighbour interactions

Equation (6) states that a metamaterial can be expressed by a Fourier series, and one can therefore realize any analytical function or dispersion relation $E(k)$ by tailoring the strength of the nonlocal interactions of different orders. Experimentally, these interaction strengths can be controlled by the connecting elements, as shown in Fig. 2a–e.

Roton-like dispersion relations. In elasticity, when only local interactions are present, one gets the textbook acoustic dispersion relation $\omega(k) \propto |\sin(ka/2)|$ with only one Fourier component[14]. Dispersion relations that contain two Fourier components resemble the roton dispersion of sound in superfluid Helium-4 (ref. 43). For small wavenumbers k, the roton dispersion relation starts as $\omega(k) \propto |k|$, followed by a maximum (the 'maxon'), a minimum (the 'roton') and a rise towards the edge of the first Brillouin zone. Richard Feynman interpreted the minimum as arising from a quasiparticle, namely, the rotation of a group of local atoms[44]. In 1965, the roton dispersion relation in Helium-4 was verified experimentally by inelastic neutron scattering[45], but over the years, further experiments and theoretical developments have refined the roton dispersion in Helium-4 (ref. 46).

Similar dispersion relations have been discussed and observed in various other correlated quantum systems at low temperature[47–49]. In classical metamaterials, roton-like dispersion relations have been obtained under ambient conditions[23,33]. The physics for the classical case can be understood from a nonlocal mass-and-spring model (Fig. 3a). To obtain two Fourier components, we consider two types of springs: one with spring constant K_1 for the nearest-neighbour connections ('local') and the other one with spring constant K_N for connection ('nonlocal') between Nth nearest neighbours (with $N = 3$ in Fig. 3). This leads to a dispersion relation following $\omega^2 = (K_1/m)\sin^2(ka/2) + (K_3/m)\sin^2(3ka/2)$, which is illustrated in Fig. 3b. It exhibits a roton-like minimum at $k \approx 2\pi/(3a)$ for sufficiently strong nonlocal interactions. This anomalous behaviour can be interpreted as arising from the hybridization of two ordinary phonon dispersion relations[21]. It leads to several unusual and interesting properties, including triple refraction owing to three coexisting Bloch states at the same frequency and broadband negative refraction[32] – theoretically at strictly zero loss[50]. Furthermore, for the wavenumber range with negative group velocity, the energy flow through the third-order nonlocal springs becomes negative[21]. In the limit of $K_3/K_1 \to \infty$, the roton-like minimum approaches zero frequency, leading to a delocalized zero mode, which is discussed subsequently.

The nonlocal strategy based on two Fourier components has been experimentally verified on different physical platforms, including elastic[23,25], acoustic[33,34] and radiofrequency systems[36] with elastic rods, acoustic channels or bayonet-Concelman (BNC) coaxial cables (Fig. 2a–e) coupling to beyond-nearest-neighbours. A stringent requirement is that the rods or channels that mediate nonlocal interactions must not overlap with each other, otherwise the interaction scheme is completely altered[32]. Periodic implementation with this constraint is more difficult in two[33] (Fig. 2d,e) and three dimensions[51] than in one dimension[21]. Anomalous refraction, however, requires two or three dimensions[32]. Nonlocal interactions can also be induced through active feedback circuits, with the advantage of tunability via an external control parameter[52].

The effective-medium theory of nonlocal systems has been investigated in many studies, particularly starting from simple discrete models[53,54], but higher-order differential equations or fractional differential equations have also been proposed[55,56]. Although most of these studies assumed only small deviations from local behaviour, the roton-like dispersion relation is connected to stronger effects of nonlocality[23]. This behaviour has successfully been captured qualitatively by effective-medium descriptions based on a higher-order differential equation with spatial derivatives up to the sixth order[23]. The effective-medium theory also qualitatively confirmed wave transmission through a nonlocal metamaterial slab[57], including bound sates in the continuum[58] that result from three coexisting Bloch states.

New avenues for topological physics. Beyond-nearest-neighbour interactions do not only change the dispersion relation of the lowest band but also lead to unusual topological properties of higher bands[35]. An example is the extended 1D Su–Schrieffer–Heeger (SSH) model, which includes third-order nonlocal interactions (Fig. 3c). Interestingly, the established approach based on the Zak phase[59] no longer correctly captures the topological properties of the system[35]. Instead, the description needs a topological winding number[60]. In contrast to a winding number of one in the standard SSH model, the extended SSH model can have a winding number of two (Fig. 3d), or a larger winding number if higher-order nonlocal

Fig. 2 | Gallery of nonlocal metamaterials based on different mechanisms. **a**–**e**, Nonlocal metamaterials based on beyond-nearest-neighbour interactions (Fig. 1). All these structures are 3D. Parts **a**–**c** are periodic along only one direction and the nonlocal interactions are mediated by rods, beams or bayonet-Concelman (BNC) cables. Part **a** is adapted from ref. 12, CC BY 4.0. Part **b** is adapted from ref. 25, CC BY 4.0. Part **c** reprinted with permission from ref. 36, Wiley. Parts **d** and **e** are periodic along two directions. The blue and red cylinders in part **d** represent third-order and fifth-order nonlocal interactions, respectively. The inset in part **e** highlights the nonlocal couplings by channels for sound. Part **d** is adapted from ref. 32, CC BY 4.0. Part **e** is adapted from ref. 33, CC BY 4.0. **f**, Nonlocal metamaterial based on delocalized zero modes. The left panel shows a finite 2D periodic structure, and the right panel shows one of its unit cells. Part **f** adapted with permission from ref. 39, APS. **g**, Nonlocal metamaterial based on chirality. The cross-shaped rods (one highlighted in red) couple the structure in a chiral manner and also mediate beyond-nearest-neighbour interactions. Part **g** adapted with permission from ref. 134, Wiley. **h**, Electric metawire with the same mechanism as in parts **a**–**e** but for nonlocal electric conduction. Thick and thin enamelled copper wires are electrically connected at soldering points (see the enlarged view at the bottom). Part **h** is adapted from ref. 38, CC BY 4.0.

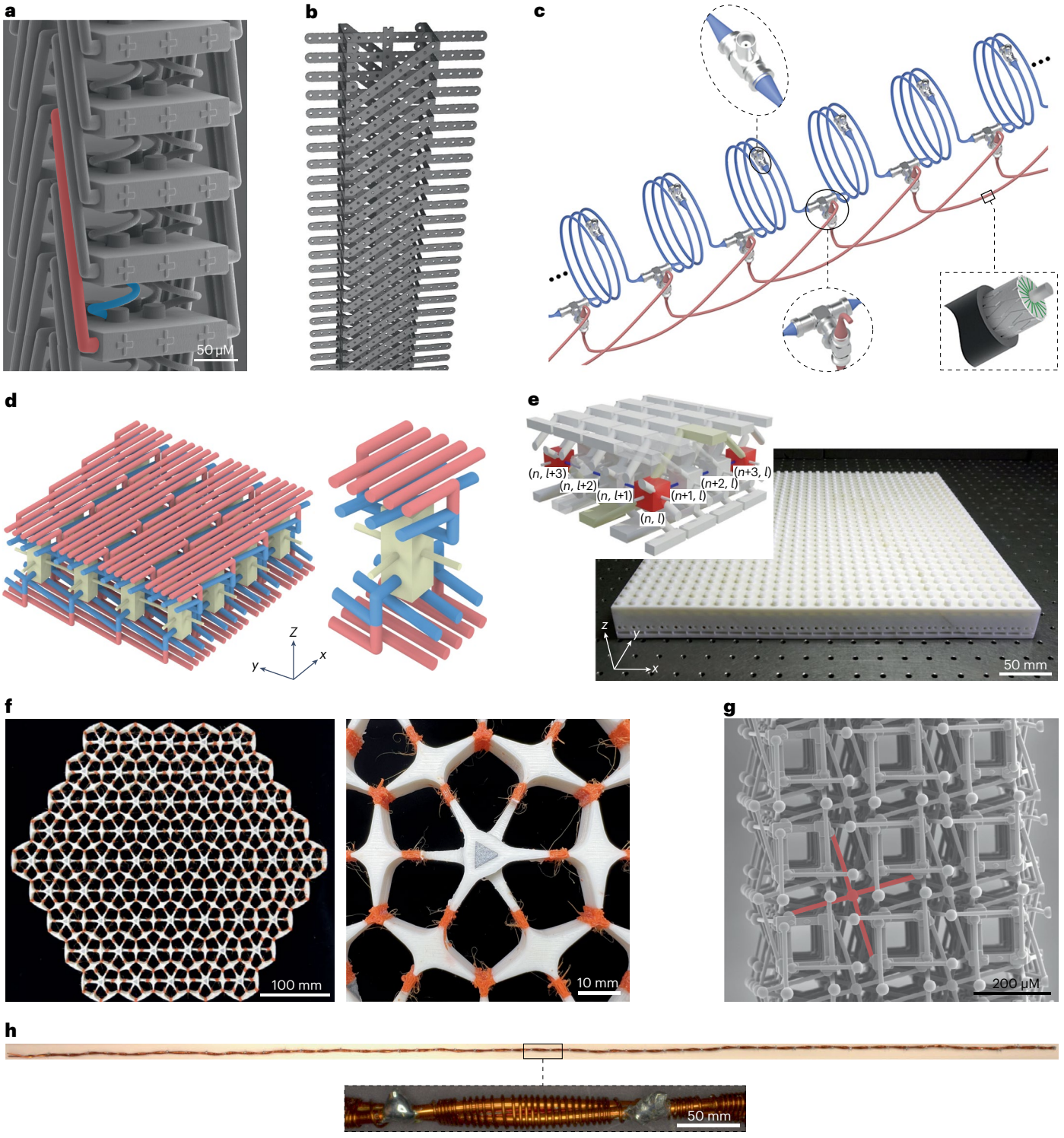

interactions are involved[35]. As a result, more edge states emerge. When calculating the number of domain-wall states between two topological phases, the winding number fails, and one needs to use the Berry connection or Jackiw–Rebbi index[61]. In 2D systems, beyond-nearest-neighbour interactions can also lead to an increased number of interface states and Dirac cones[62]. Furthermore, nonlocal interactions can enable specific higher-order topological states, such as 0D corner states[63–65]. This has been observed in photonic kagome lattice of dielectric cylinders[64]. The corner states can only be explained if the next-nearest-neighbour couplings are accounted for in a tight-binding model[64]. Yet, more complex behaviours are expected for higher-order nonlocal interactions.

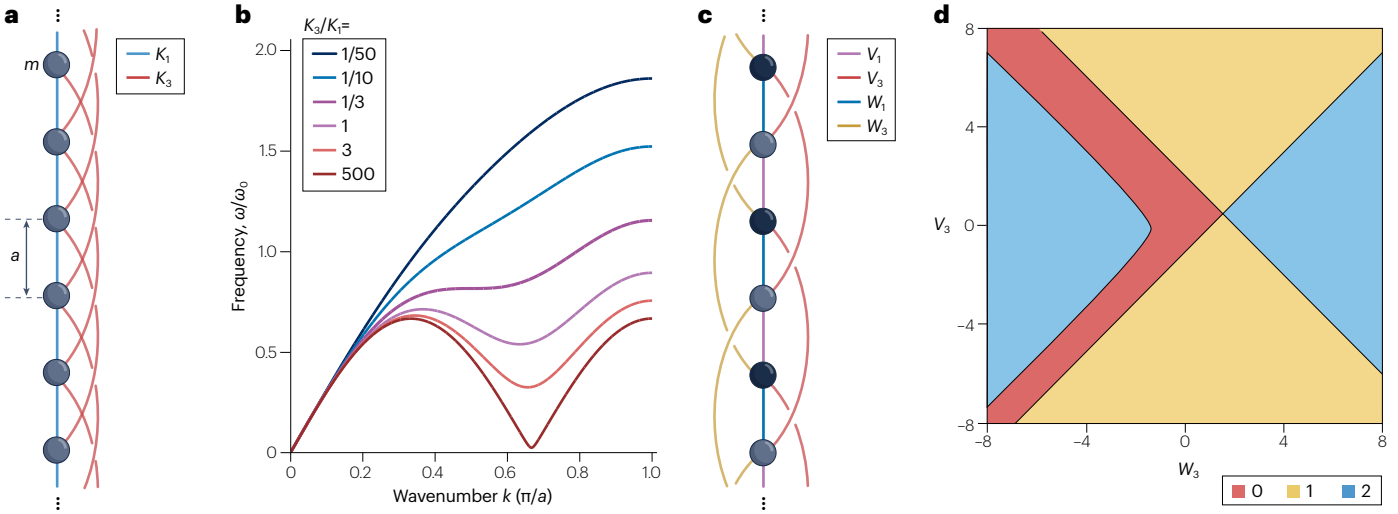

Fig. 3 | Beyond-nearest-neighbouring interactions for tailoring dispersion bands and topological properties. a, A 1D mass-and-spring model with nonlocal interactions for roton-like bands. Each mass (grey circles) is coupled to their immediate neighbours by springs (blue lines), with spring constant K_1, as well as to their third-nearest-neighbours by springs (red lines), with spring constant K_3. **b**, Phonon bands for the nonlocal model in part **a**. Roton-like band, featured with a local minimum on the band, is obtained for strong nonlocal interactions. Part **a** is adapted from ref. 21, CC BY 4.0. **c**, Extended Su–Schrieffer–Heeger tight-binding model with third-order nonlocal interactions (red and yellow lines). **d**, Winding numbers of the model in part **c** with $w_1 = -0.5$, $v_1 = -1.5$ and different combinations of nonlocal interaction strength. A maximal winding number of 2 instead of 1 for the standard Su–Schrieffer–Heeger model can be obtained. Part **d** reprinted with permission from ref. 35, APS.

Delocalized zero modes

To understand what a delocalized zero mode is and how it leads to nonlocality, let us consider the pantographic mechanical structure[66–68] (Fig. 4a), which is inspired by pantographs or scissor mechanisms. All struts (straight lines) are coupled by hinges (open blue circles) such that an angle change on the left-hand side is transferred to the right-hand side, which is a highly nonlocal response. For ideal hinges and rigid struts, this transfer requires zero energy, even over very large distances, corresponding to a delocalized zero mode. Mathematically, a delocalized zero mode is a Bloch-wave mode with a well-defined Bloch vector $\mathbf{k}_{zm}$ that can be excited with strictly zero energy. It is fundamentally different from the Guest–Hutchinson zero modes[69–71] in many mechanical systems with insufficient connectivity, such as 2D mechanical square lattices or kagome lattices composed of masses and springs[72–74]. These systems host an infinite number of zero modes across extended regions in reciprocal space[39]. As localized zero modes at any location can be constructed from these zero modes, a local perturbation cannot propagate to a distant location.

Anomalous cones. A delocalized zero mode can create an anomalous cone at $\mathbf{k}_{zm}$ in reciprocal space (Fig. 4b), owing to the continuity of frequencies versus wavenumbers. The cone is anomalous in the sense that the zero mode is different from trivial zero modes at $\mathbf{k} = \mathbf{0}$, which represent rigid translations in mechanics or homogeneous optical fields in vacuum. Anomalous cones can be used to achieve broadband negative refraction even down to the static frequency range (see Fig. 4b for a dispersion relation and Fig. 4c for selected iso-frequency contours)[39,75]. For electromagnetism, it has been shown that such behaviour cannot be achieved for a purely local medium[50,76]. For anomalous cones shifted to non-zero wavenumber, orientation-dependent coupling to an ordinary background material leads to enhanced directional emission[75]. Additionally, metamaterials with anomalous cones constitute a platform for Weyl physics that is much more controllable and that makes experiments easier than for atomic materials[73]. Spatially confined locally resonant modes can become extended or delocalized through coupling via multiple scattering or by hybridization with propagating modes. This enables interesting phenomena such as negative refraction and topological wave behaviours[77–79]. However, these properties are typically limited to a narrow frequency range close to the local resonance frequency.

Delocalized zero modes and anomalous cones have extensively been studied in mechanics[72,73]. The resulting metamaterials generally rely on small tips to approximate ideal hinges (see Fig. 2f as one example). A recent design strategy is based on 'oligomodal' mechanical metamaterials[80], which host a fixed number of zero modes irrespective of system size. A method based on directed graphs has been proposed to analyse these zero modes and to design anomalous cones at any wavenumber in reciprocal space[13,39].

A second method is based on a special type of elastic materials whose elasticity matrices have one or more zero eigenvalues[81–84]. Each zero eigenvalue leads to an easy mode, or specifically to a strain state that induces zero elastic strain energy. Elastic materials with easy modes can be realized by solid microstructures[85–89]. The kagome lattice mentioned earlier is an example[72,90,91]. In materials with easy deformation modes, Bloch modes along one or more wavevector directions have zero frequency[92]. A single Bloch mode at an isolated wavenumber can be obtained by supercell-induced band-folding[93]. Alternatively, distortions can be introduced into these materials to eliminate excessive zero modes[72,73]. This approach has been used to achieve mechanical Weyl points, although the cone location cannot easily be predicted and adjusted[73].

Interlaced wire media have been used to obtain anomalous cones in electromagnetism[94–97]. Normally, a simple cubic mesh grid of wires

has no dispersion band emerging from zero frequency because all wires have the same electric potential in the low-frequency limit and only the trivial solution of zero electric field is allowed. However, the situation becomes drastically different for two disconnected copies of a mesh grid, also referred to as non-Maxwellian media[95]. In such metamaterials, Bloch modes starting from zero frequency occur[75]. The Bloch modes originate from the potential difference between the two (or more) mesh grids and share similarities with the propagating modes between two parallel metal plates. The location in k-space and the number of anomalous cones can be controlled by the connectivity of wire mesh[75]. The analogy of this concept for elastic waves was discussed in ref. 13.

Frozen evanescent modes. In real-life metamaterials, perturbations generally lift the zero-frequency minimum of the anomalous cones to a minimum at finite frequencies (Fig. 4d). Thus, at first sight, no zero-frequency modes or waves seem to occur. However, evanescent modes with complex-valued wavenumbers still exist.

To appreciate this general behaviour, consider a local parabolic minimum of the dispersion relation as an example (Fig. 4d). This dispersion relation can be Taylor-expanded around the local minimum $(k_{\min}, \omega_{\min})$ as $\omega \approx \omega_{\min} + \zeta \Delta k^2$ with $\zeta > 0$ and $\Delta k = k - k_{\min}$ (refs. 98,99). As a result, two branches emerge from the local minimum and bend towards lower frequency[12]. These two branches lead to two Bloch modes with strictly zero frequency (dots in Fig. 4d) and complex conjugated wavenumbers $k_{zm} = \mathrm{Re}(k_{zm}) \pm \mathrm{i}\mathrm{Im}(k_{zm}) \approx k_{\min} \pm \mathrm{i}\sqrt{\omega_{\min}/\zeta}$. These static or 'frozen' Bloch modes are evanescent waves with a spatial oscillation period of $2\pi/|\mathrm{Re}(k_{ZM})|$ and an exponential decay length of $l = 1/|\mathrm{Im}(k_{zm})| \approx \sqrt{\zeta/\omega_{\min}}$, which diverges as $\omega_{\min}$ approaches zero frequency. These additional bands and the corresponding frozen evanescent modes (Fig. 4e) have been demonstrated in a nonlocal

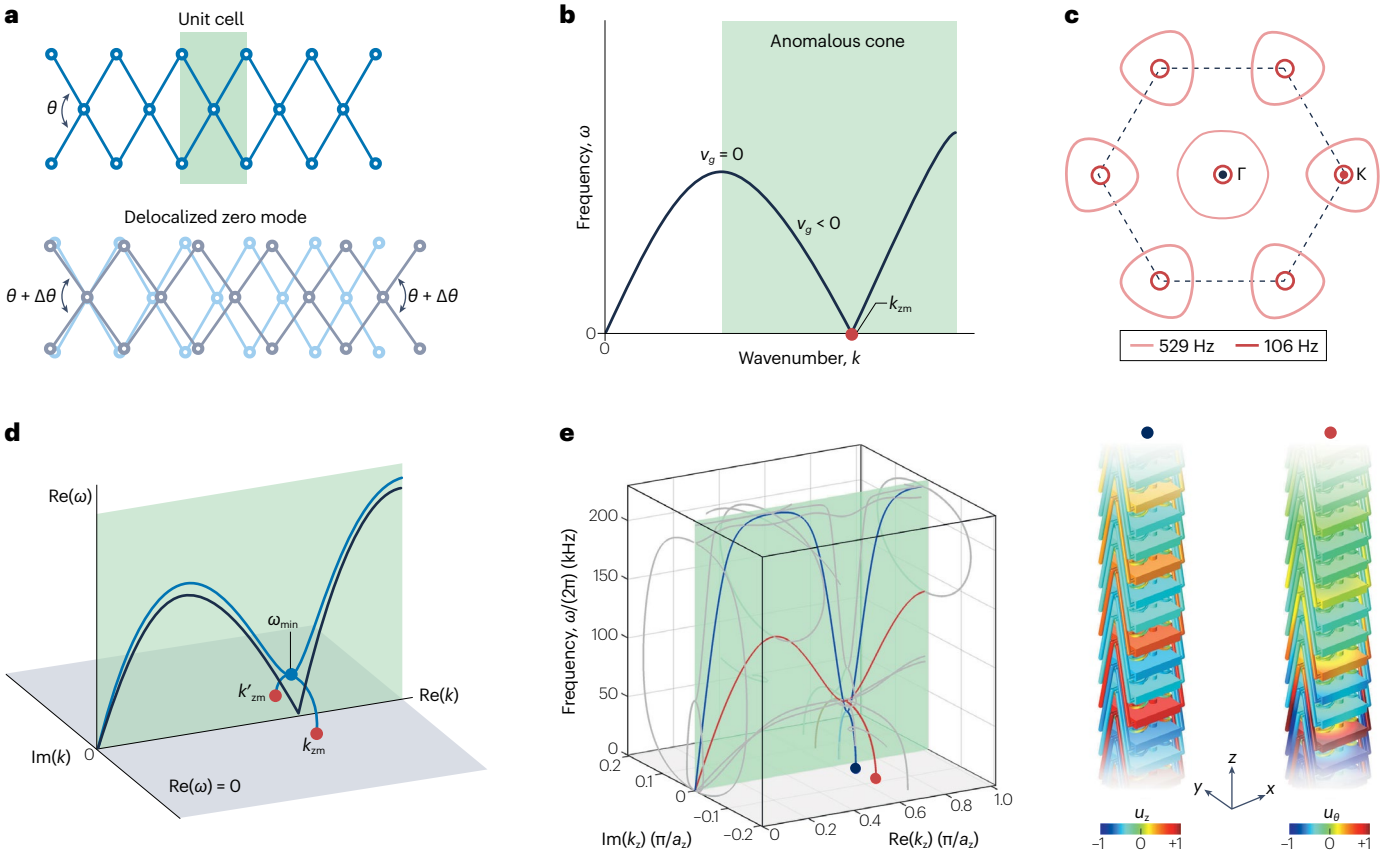

Fig. 4 | Delocalized zero modes for nonlocality. a, A 1D pantographic structure consists of struts (straight lines) coupled by hinges (open blue circles). For the case of ideal hinges and rigid struts, the bottom panel depicts a delocalized zero mode of the structure, in which the angle between two adjacent struts in each unit cell increases by the same amount. The deformation mode is a delocalized zero mode, a Bloch mode with Bloch wavenumber $k_{ZM} = 0$. The zero mode enables transfer of an angle (θ) change between the two left-most struts to the two right-most struts of a finite-size periodic structure – a highly nonlocal behaviour. For non-ideal hinges and/or non-rigid struts, the transfer of angle change is no longer perfect, yet nonlocal behaviour persists. **b**, An anomalous cone, highlighted by the green shading, naturally emerges from the wavenumber, k_{zm}, of a delocalized zero mode. Zero group velocity ($v_g = 0$) and negative group velocity ($v_g < 0$) can arise at certain wavenumber. **c**, Iso-frequency contours of the metamaterial shown in Fig. 2f with a delocalized zero mode at $\mathbf{k}_{zm} = \mathbf{K}$. **d**, In actual metamaterials, the ideal anomalous cone (black line) is modified (blue line), leading to a local minimum (blue circle) at finite frequency. In the complex wavenumber space, two complex-valued bands, with real-valued frequencies but complex-valued wavenumbers, start from the local minimum, ω_{min}, and lead to evanescent modes at zero frequency (red circles) – frozen evanescent Bloch waves, with complex-valued wavenumbers k_{zm} and k'_{zm}. The grey plane and green plane correspond to $\mathrm{Re}(\omega) = 0$ and $\mathrm{Im}(k) = 0$, respectively. **e**, Complex-valued band structures of the nonlocal metamaterial beam shown in Fig. 2a. Right panels show the displacement fields for the longitudinal evanescent mode (blue circle in part **e**) and torsional evanescent mode (red circle in part **e**). The green plane corresponds to $\mathrm{Im}(k) = 0$. Part **e** is adapted from ref. 12, CC BY 4.0.

metamaterial beam[12]. The frozen evanescent modes (Fig. 4e) clearly show spatially oscillatory and exponentially decaying profiles.

Such frozen evanescent modes emerging from some local minimum in the dispersion relation are common for crystals and metamaterials[100–103]. However, they are often not relevant for two reasons. First, their decay length is often extremely short and on the scale of one period or lattice constant of the system. This means that only the last atoms or meta-atoms at the edge of the sample are affected. Second, the corresponding spatial modes may be complicated and exhibit intricate spatial distributions, such that one cannot couple to these modes under ordinary conditions.

By contrast, frozen evanescent modes with large decay lengths can lead to pronounced anomalous static responses reaching deep into the bulk of a sample[12]. For example, when stretching an ordinary elastic beam with finite length, the displacement simply increases linearly from one end to the other. In sharp contrast, nonlocal metamaterial beams can exhibit strong spatial oscillations arising from frozen evanescent phonon modes[12]. The resulting displacement fields depend on the boundary loading, leading to a violation of Saint-Venant's principle in mechanics[104] with potential applications in remote sensing[12]. Moreover, two or more frozen evanescent phonon modes can lead to constructive or destructive interference of the displacement field in the middle of the beam, depending on the length of the beam. This behaviour is similar to Fabry–Pérot resonances in a cavity at finite frequencies, but the frozen modes or waves we consider here are purely static. As a result of these interferences, the effective spring constant of a metamaterial beam can oscillate with respect to the beam length[12], whereas ordinarily, the spring constant scales inversely with beam length. This ordinary behaviour is only recovered if beam length exceeds around twice the decay lengths of the frozen evanescent modes[12].

Mathematically, frozen evanescent modes are special solutions of differential equations with spatial derivatives up to the second order. Therefore, they can arise in many different physical systems[101–103]. An example quite different from elasticity is electric conduction. In an electric metawire (Fig. 2h) with nonlocal connections[38], the resistance between two points on the wire does not scale proportional to distance[38], but again oscillates like the spring constant of a metamaterial beam[12] discussed earlier. We expect anomalous thermal conduction to behave analogously in the presence of nonlocality. However, diffusion-type problems[105] are generally not mathematically equivalent to elasticity[106].

The concept of frozen evanescent modes is a general approach to understand and determine characteristic lengths in static problems[107]. In generalized effective-medium descriptions of elasticity, characteristic lengths have been investigated for many years[108–110], but there was no systematic approach how to extract them from a known periodic microstructure. Examples include the push-to-twist coupling in 3D chiral materials[40,111,112], the stretch-to-bending coupling in 2D chiral metamaterials[113,114] and metamaterials with anomalous stretching behaviours[115,116].

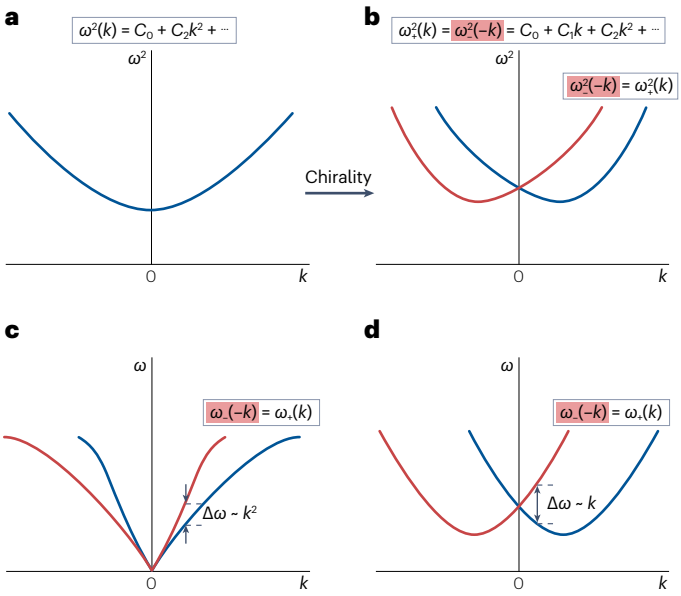

Fig. 5 | Frequency splitting resulting from chirality. a, The squared frequency dispersion $\omega^2(k)$ of a passive achiral system only contains even-order terms in k. **b**, Bands for chiral systems can exhibit odd-order terms in k, but must occur in pairs according to $\omega_\pm^2(k) = C_0 \pm C_1k + C_2k^2 \pm C_3k^3 + \ldots$ owing to time-reversal symmetry. Chirality leads to a weak quadratic frequency splitting $|\omega_+ - \omega_-| \sim k^2$ between two chiral bands starting from zero frequency (part **c**), or stronger linear splitting $|\omega_+ - \omega_-| \sim k$ between two higher bands (part **d**).

Chirality

As discussed in the introduction (equation (6)), for achiral media, by spatial symmetry, only even-order terms occur in the dependence on wavenumber k. In the presence of chirality, even and odd terms can occur, enhancing the possibilities of designing dispersion relations of waves in metamaterials. However, in the presence of time-reversal symmetry and for passive systems, the dispersion relations $\omega(k)$ (Fig. 5a) must be symmetric with respect to the wavenumber k (ref. 5). Therefore, bands containing odd-order terms of k must occur as pairs $\omega_\pm^2(k) = C_0 \pm C_1k + C_2k^2 \pm C_3k^3 + \ldots$, with constants C_0, C_1… (Fig. 5b). Note that for classical waves, the squared frequency ω^2 plays a similar role to energy (equation (6)) for quantum systems. Each of the two bands alone has no inversion symmetry, $\omega_+(-k) \neq \omega_+(+k)$. However, the two bands combined satisfy time-reversal symmetry: $(\omega_+^2(-k), \omega_-^2(-k)) = (\omega_-^2(+k), \omega_+^2(+k))$. This behaviour holds for the lowest bands (for example, acoustic phonons) and for higher bands (such as optical phonons). The odd-order terms result in frequency splitting between the two bands $|\omega_+(k) - \omega_-(k)| \neq 0$, leading to unique nonlocal properties that cannot be achieved with the two approaches discussed thus far[117–123].

Optical activity and acoustical activity. Optical activity results from the frequency splitting between the two lowest transverse bands in chiral optical media[7]. The waves corresponding to these bands are circularly polarized left-handed and right-handed electromagnetic waves. Their phase velocities are different owing to the discussed frequency splitting. This difference gives rise to the phenomenon of optical activity, for which the polarization direction of a linearly polarized incident transverse electromagnetic wave gradually rotates as it propagates through the chiral material[7]. The counterpart of optical activity for acoustic waves (or phonons) in solids is acoustical activity[117,120], where two circularly polarized transverse elastic waves replace the electromagnetic waves.

Although optical activity and acoustical activity are generally weak in natural chiral materials, they can become very large in metamaterials[118,119]. Suppose we Taylor-expand the two dispersion relations

according to $\omega_{\pm}^2(k) = C_2k^2 \pm C_3k^3 + \ldots$, as they start from the zero frequency and cannot be negative. The frequency splitting is at most of second order, $|\omega_+(k) - \omega_-(k)| \sim k^2$ (Fig. 5c). Nevertheless, artificially designed metamaterials can exhibit orders of magnitude stronger chiral effects, such as tens of degrees change in the polarization direction over a single metamaterial lattice constant[120]. Natural chiral crystals and most chiral metamaterials are highly anisotropic and only support purely circularly polarized eigenmodes along selected high-symmetric directions. For specially designed metamaterial crystals, degeneracies can be enforced by design[122,123], and for quasi-crystalline metamaterial lattices, isotropy is enforced on average[121]. Both approaches allow obtaining purely circularly polarized eigenmodes for all wave propagation directions in 3D space.

Both optical activity and acoustical activity have been successfully modelled by effective-medium descriptions[124,125]. In optics, cross-coupling parameters or chiral parameters can be introduced into the constitutive matrix that couples (**D, B**) and (**E, H**) to model optical activity[125]. For elasticity, one choice is to use a wavenumber-dependent Cauchy elastic tensor[124], again corresponding to spatial dispersion. An alternative and more suitable approach is to use micropolar continuum theory[126], which assigns additional microrotation degrees of freedom to each material point in addition to the usual translational degrees of freedom. In this case, acoustical activity is modelled by similar cross-coupling terms in the constitutive matrix as in optics. For both optics and acoustics, the magnitude of the cross-coupling parameters is bounded by the main-diagonal terms in the constitutive matrix, resulting from the requirement of positive energy[126]. A third choice is Willis effective-medium theory, in which momentum and stress are coupled with strain and velocity[127–129].

A chiral effect that has no counterpart in optics is the push-to-twist coupling in chiral elastic solids[40], which stems from the chirality-induced coupling between a twist mode and a longitudinal mode. The latter is generally absent in electromagnetic materials. Micropolar effective-medium theory can also model this chiral effect[126].

Chirality-induced frequency splitting for higher bands. For higher bands, the chirality-induced frequency splitting can be more pronounced than for the lowest bands[125]. Starting from the expansion $\omega_{\pm}^2(k) = C_0 \pm C_1k + C_2k^2 + \ldots$, we see that a linear (rather than quadratic) frequency splitting according to $|\omega_+(k) - \omega_-(k)| \sim |k|$ is expected. For small wavenumbers, one band has a negative group velocity, and the other a positive group velocity (Fig. 5d). This offers a route for obtaining negative refraction, as first discussed in optics[130–132]. For mechanics, yet more pronounced effects were suggested based on micropolar elasticity[133]. Here, the higher optical phonon bands split owing to chirality and hybridize with the acoustic phonons, leading to a roton-like dispersion relation of the lowest bands[133]. Corresponding metamaterials have been designed and studied[134]. In this structure, the nonlocal couplings are directly visible by the rods marked in red in Fig. 2g. It is presently not clear whether such pronounced effects of chirality and nonlocality can also be obtained in optics. In fluids, such as air or water, only longitudinal acoustic waves are supported, but no transverse waves. Therefore, not all of the above can simply be translated. However, effective transverse air sound in metamaterials can be achieved by using dipole modes to mimic transverse displacements in solids[135]. Furthermore, negative refraction resulting from the chiral splitting of higher bands can be achieved for airborne sound[135].

Time dependence

Metamaterials generally rely on intentional material inhomogeneity in space to manipulate waves[136,137]. Recently, it has been pointed out that material inhomogeneity in time can also be harnessed to control waves[138–140]. Here, material properties can experience step-like changes in time[141]. Interestingly, this approach can also lead to nonlocal behaviour[142]. A simple example is the propagation of an optical pulse in a homogeneous material with an electric permittivity, ε_0, that changes to a different value, $\varepsilon(t) \neq \varepsilon_0$, in a very short-time interval, $0 < t < \tau$ and then changes back to ε_0. At the two temporal interfaces of $t = 0$ and $t = \tau$, the pulse is partially reflected and partially refracted, similar to the reflection and refraction of a pulse at a spatial interface separating two media. This effect has been referred to as time reflection and time refraction[142]. It should be noted that, at a spatial interface, the frequency is conserved and the wavenumber changes, whereas the opposite holds true at a temporal interface[141]. Interference occurs between the time-reflected and time-refracted signals at the two temporal interfaces, leading to a wavenumber dependence of the total reflection and refraction coefficients. This dispersive response depends on the duration τ of the modulation and the modulation shape (discontinuous or smeared step)[142]. This behaviour resembles the propagation of a wave through a slab of time-independent material exhibiting nonlocality[143].

The main technical challenges for experiments are three aspects, particularly for optical signals: the abrupt change of material properties must be large; the jump of the material properties should be quick, at least comparable with the period of the waves; the modulation must be well synchronized throughout the medium. At present, microstrip lines for radiofrequency waves constitute a suitable platform[144]. The available control frequency has increased from tens of megahertz to sub-gigahertz by using optically controlled picosecond-switchable photodiodes[145]. Acoustic or elastic experiments in the sub-kilohertz frequency range are also beginning to emerge[146,147].

Nonlocal metasurfaces

A metasurface can spatially and temporally shape waves that impinge on it from air or another medium, which are reflected or transmitted. The metasurface acts like a generalized phase plate[148–150] or a generalized diffractive optical element[151]. Unlike for the metamaterials discussed earlier, the units of a metasurface are not necessarily arranged periodically. To accomplish wavefront shaping, the wave must locally acquire a phase shift between 0 and 2π, equivalent to a thickness between zero and one wavelength. However, as the wavelength is not a preserved quantity, it may be (much) smaller than the wavelength in the outside medium. The community therefore often speaks about 'sub-wavelength' thicknesses or 'flat' optics[150]. This approach has achieved various interesting functions, including anomalous beam deflections following a generalized version of Snell's law[152] and focusing.

Metasurfaces are often local in the sense that their unit cells are designed independently under conditions for which the interaction with neighbouring unit cells is negligible, which corresponds to ignoring the effects of spatial dispersion. This assumption does not only decrease the efficiency of local metasurfaces but also limit the possibilities of controlling waves[19]. For example, to deflect an incident beam by a large angle with 100% energy efficiency, the local transmission cannot be 100% everywhere along the metasurface[153]. Energy flow in directions parallel to the metasurface is inevitable for perfect transmission[154,155], which means nonlocality is a must. Interestingly, this restriction can be relaxed for curved metasurfaces[156]. In principle, all metasurfaces

exhibit a finite degree of nonlocality as the scattering of the unit cells cannot be ideally localized[19]. By deliberately exploiting and enhancing nonlocal interactions, metasurfaces allow to perform more complex functions[19], such as taking spatial derivatives of incident images[157].

As nonlocal metasurfaces for optics and acoustics have been covered in recent reviews[18–20], we focus on recent progress here. In the following, we introduce nonlocal metasurfaces according to two different mechanisms, namely, leaky-wave modes and physical couplings. Leaky-wave modes have mainly been used in optics, whereas physical couplings have been exploited in acoustics and elasticity.

Leaky-wave modes

Leaky-wave modes are localized in the direction perpendicular to the metasurface but are extended within the plane of the metasurface[158], thereby laterally coupling unit cells of the metasurface (Fig. 6a). We point to the analogy to zero modes in nonlocal metamaterials discussed earlier (Fig. 4a). Various approaches to control nonlocality and leaky-wave modes have been covered in two previous reviews[18,19]. More recently, nonlocal couplings have also been tailored by adjusting the unit-cell period[159] (Fig. 6b) or tuning the height of plasmonic scatters[160].

Generally speaking, nonlocal metasurfaces exhibit wavenumber-dependent transmission, enabling more powerful functions than beam deflection[19]. A prominent example is to perform spatial derivatives of incident images, enabling fast and energy-efficient image (pre-) processing[19], for example, for edge detection. Another example is to compress the space between lenses in optical systems, leading to more compact optical devices[161–163]. A recent example is the combination of spatial differentiation and temporal differentiation[164,165]. Here, the nonlocal metasurface is activated only when signals change substantially in time, thus achieving event-based processing[166].

The high frequency selectivity of nonlocal metasurfaces[167] is another advantage compared with more traditional phase masks. This means that a designed function works only at a targeted frequency or in a narrow frequency range[168] (Fig. 6c). This frequency selectivity is attractive for augmented reality[169], where visible light from the environment can perfectly pass through a metasurface. By combining the leaky modes of different nonlocal metasurfaces, multiple images at selected colours can be superimposed onto the environment.

Physical coupling

Nonlocal interactions for acoustic and elastic metasurfaces are more often achieved by physical connections[20], which are quite similar to what we discussed for nonlocal metamaterials (Fig. 2a–e). This strategy inevitably complicates the structure design to support nonlocal couplings in the plane of the metasurface[170] (Fig. 6d). Yet, this has been the main approach to design various nonlocal acoustic and

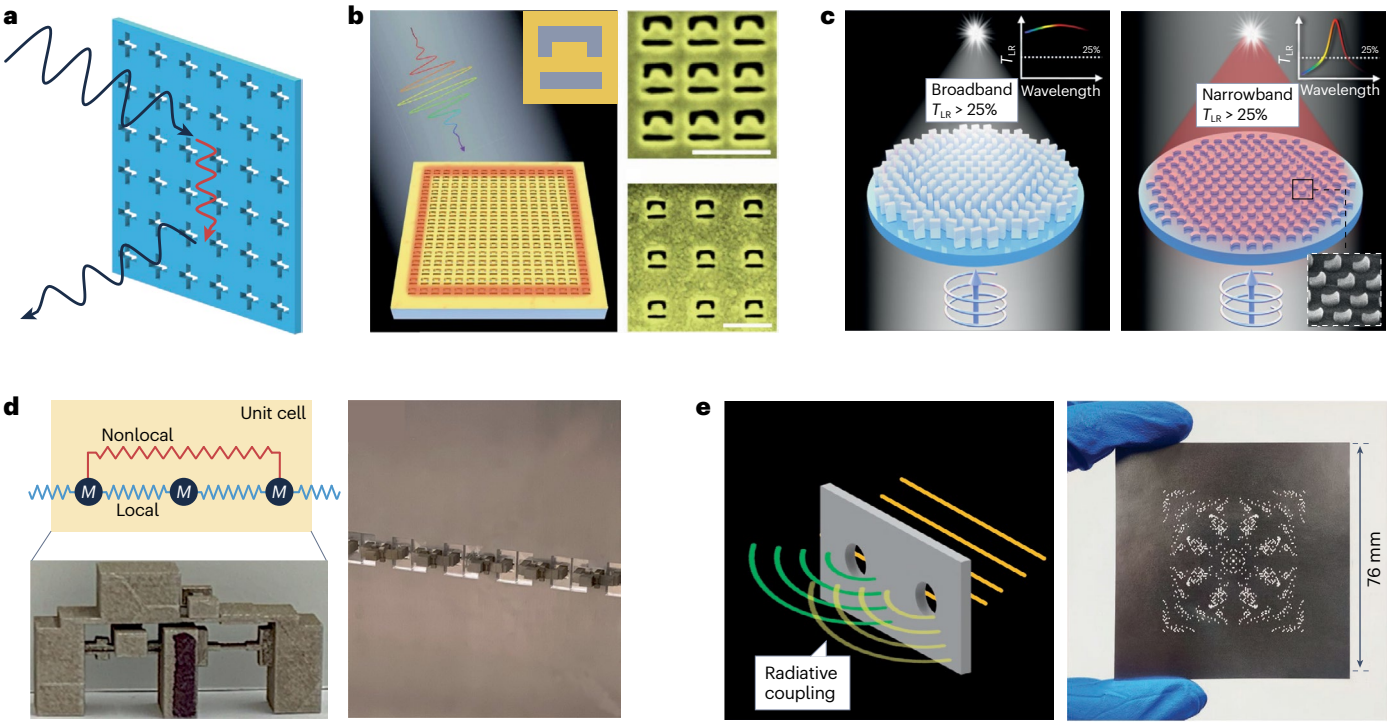

Fig. 6 | Nonlocal metasurfaces. a, Nonlocality for optical metasurfaces mainly results from leaky-wave modes (red) propagating within the metasurface plane. Incident and reflected light is shown in black. **b**, A simple method of tuning nonlocal coupling is to vary the unit cell size. White scale bars, 500 nm. Part **b** adapted with permission from ref. 159, AAAS. **c**, A local metasurface (left panel) focuses waves with low frequency selectivity. A nonlocal optical metasurface (right panel) can focus light selectively only for a targeted narrow frequency range. The conversion efficiency can be enhanced by Huygens' nonlocality. Part **c** adapted from ref. 168, Springer Nature Limited. **d**, A nonlocal mechanical metasurface based on beyond-nearest-neighbour couplings. The left top panel is a schematic of the metasurface unit cell (left bottom panel). Right panel is a metasurface composed of multiple unit cells. Bottom left panel and right panel of part **d** adapted with permission from ref. 170, PNAS. **e**, Nonlocal couplings in acoustics can be directly realized via radiative coupling between acoustic waves transmitted through different holes in a screen. The right panel shows an ultra-thin nonlocal acoustic metasurface based on a perforated plate. Right panel of part **e** is adapted from ref. 176, CC BY 4.0.

Glossary

Characteristic length scales
For sample sizes much larger than the characteristic length, size effects become negligible.

Chiral metamaterials
A metamaterial lacking inversion symmetry, mirror planes and rotation–reflection symmetries.

Interlaced wire media
An electromagnetic structure composed of interconnected metal wire meshes.

Non-Bloch solutions
Non-Bloch solutions do not obey Bloch's theorem but are still solutions of the periodic problem.

Saint-Venant's principle
The linear elastic response of a material in the far field becomes insensitive to the precise location and distribution of the loading.

Size effects
We refer to size effects as the dependence of material properties, for example, the Young's modulus, on the size of the sample.

elastic metasurfaces[171–175]. For underwater metasurfaces, nonlocality is often inevitable owing to strong coupling between the water-borne sound and the components of the metasurface, even without physical channels to couple different unit cells[173,176].

Generally, it is fair to say that the development of nonlocal metasurfaces for acoustics and elasticity lags behind their optical counterpart. Typical functions such as anomalous reflection, beam splitting or focusing have been demonstrated[20]. A more recent application is a nonlocal acoustic hologram[173,176], which can potentially be used for particle or cell manipulation and trapping. Here, the wave transmitted through a metasurface forms a desired field pattern at an image plane. Instead of using channels to couple the metasurface unit cells, nonlocality can solely arise from radiative coupling between transmitted waves at different locations[176] (Fig. 6e). This type of coupling has been exploited to design ultra-thin nonlocal metasurfaces based on perforated plates[176]. Nonlocal interactions can be further enhanced by using the vibration of the thin perforated plate itself, particularly for underwater sound[173]. Further examples of nonlocal metasurfaces for acoustics and elasticity are emerging, such as performing nonlocality-enabled spatial derivatives with elastic waves[174] or using nonlocal metasurfaces for hyperbolic wave propagation[177].

Outlook

Local metamaterials and metasurfaces[1,2,150] have long exploited frequency-dependent effective responses to control and manipulate electromagnetic, elastic and acoustic waves. Frequency dependences inherently come with fundamental restrictions owing to the Kramers–Kronig relations, arising from causality[178]. Nonlocal metamaterials and metasurfaces additionally exploit wavenumber-dependent effective responses. Translated from reciprocal space to real space, this means that one must design, control and enhance the strengths of nonlocal couplings between the unit cells or building blocks of metamaterials and metasurfaces. In this Review, we have summarized different approaches in different classical systems to achieve such coupling control.

Interestingly, nonlocality also represents a path towards controlling strictly static effective behaviours of metamaterials via frozen evanescent waves with anomalously long spatial decay lengths[12]. Such characteristic decay lengths have previously been discussed — for example, in the framework of generalized effective-medium elasticities — but have remained somewhat obscure and without any connection to the dynamic band structure of the effective medium. Frozen (or zero-frequency) evanescent Bloch waves arising from pronounced nonlocality even reach into diffusion problems such as electrical conduction and Ohm's law, which are not usually associated with waves.

Combining controlled nonlocality with non-Hermitian systems or with non-reciprocal systems may enable further unusual or exotic behaviours such as fundamentally different versions of the skin effect[179]. One often wishes to reduce the system thickness to a minimum, for example, for applications in mobile phones, but there is a limit to how thin functional devices can be. Recently, the concept of overlapping nonlocality has been identified as the key reason for the finite minimum thickness of optical systems targeting specific optical functions[180]. Although the connection is not perfectly clear yet, recent theoretical studies[181,182] suggest that nonlocal metamaterials and metasurfaces may make a distinct contribution to thin and therefore compact optical systems in the future, perhaps also including optical neural networks[183].

Published online: 16 May 2025

References

1. Kadic, M., Milton, G. W., van Hecke, M. & Wegener, M. 3D metamaterials. *Nat. Rev. Phys.* **1**, 198 (2019).
2. Bertoldi, K., Vitelli, V., Christensen, J. & van Hecke, M. Flexible mechanical metamaterials. *Nat. Rev. Mater.* **2**, 1 (2017).
3. Li, Y. et al. Transforming heat transfer with thermal metamaterials and devices. *Nat. Rev. Mater.* **6**, 488 (2021).
4. Zhang, Z. et al. Diffusion metamaterials. *Nat. Rev. Phys.* **5**, 218 (2023).
5. Landau, L. D. et al. *Electrodynamics of Continuous Media* (Elsevier, 2013).
6. Milton, G. W. *The Theory of Composites* (Cambridge Univ. Press, 2002).
7. Barron, L. D. *Molecular Light Scattering and Optical Activity* (Cambridge Univ. Press, 2004).
8. Bliokh, K. Y., Leykam, D., Lein, M. & Nori, F. Topological non-Hermitian origin of surface Maxwell waves. *Nat. Commun.* **10**, 580 (2019).
9. Zhang, Z., Delplace, P. & Fleury, R. Superior robustness of anomalous non-reciprocal topological edge states. *Nature* **598**, 293 (2021).
10. Chen, Q. et al. Anomalous and Chern topological waves in hyperbolic networks. *Nat. Commun.* **15**, 2293 (2024).
11. Van Mechelen, T. & Jacob, Z. Universal spin-momentum locking of evanescent waves. *Optica* **3**, 118 (2016).
12. Chen, Y. et al. Anomalous frozen evanescent phonons. *Nat. Commun.* **15**, 8882 (2024).
13. Bossart, A. A. *Nonlocally-Resonant Metamaterials* (EPFL, 2023).
14. Kittel, C. & McEuen P. *Introduction to Solid State Physics* (Wiley, 1996).
15. Ciracì, C. et al. Probing the ultimate limits of plasmonic enhancement. *Science* **337**, 1072 (2012).
16. Monticone, F. et al. Roadmap on nonlocality in photonic materials and metamaterials. *Opt. Mater. Express* https://doi.org/10.1364/OME.559374 (2025).
17. Alibert, J. & Seppecher, P. Closure of the set of diffusion functionals — the one dimensional case. *Potential Anal.* **28**, 335 (2008).
18. Overvig, A. & Alù, A. Diffractive nonlocal metasurfaces. *Laser Photon. Rev.* **16**, 2100633 (2022).
19. Shastri, K. & Monticone, F. Nonlocal flat optics. *Nat. Photon.* **17**, 36 (2023).
20. Wang, X., Dong, R., Li, Y. & Jing Y. Non-local and non-Hermitian acoustic metasurfaces. *Rep. Prog. Phys.* https://doi.org/10.1088/1361-6633/acfbeb (2023).
21. Chen, Y., Kadic, M. & Wegener, M. Roton-like acoustical dispersion relations in 3D metamaterials. *Nat. Commun.* **12**, 3278 (2021).
22. Fleury, R. Non-local oddities. *Nat. Phys.* **17**, 766 (2021).
23. Julio-Andrés, I. et al. Experimental observation of roton-like dispersion relations in metamaterials. *Sci. Adv.* **7**, m2189 (2021).
24. Cui, J., Yang, T., Niu, M. & Chen, L. Tunable roton-like dispersion relation with parametric excitations. *J. Appl. Mech.* **89**, 111005 (2022).
25. Chaplain, G. J., Hooper, I. R., Hibbins, A. P. & Starkey, T. A. Reconfigurable elastic metamaterials: engineering dispersion with beyond nearest neighbors. *Phys. Rev. Appl.* **19**, 44061 (2023).

26. Sepehri, S., Mashhadi, M. M. & Fakhrabadi, M. M. S. Nonlinear nonlocal phononic crystals with roton-like behavior. *Nonlinear Dyn.* **111**, 8591 (2023).
27. Zhao, C., Zhang, K., Zhao, P., Hong, F. & Deng, Z. Bandgap merging and backward wave propagation in inertial amplification metamaterials. *Int. J. Mech. Sci.* **250**, 108319 (2023).
28. Kazemi, A. et al. Drawing dispersion curves: band structure customization via nonlocal phononic crystals. *Phys. Rev. Lett.* **131**, 176101 (2023).
29. Guarracino, F., Fraldi, M. & Pugno, N. M. Local-to-non-local transition laws for stiffness-tuneable monoatomic chains preserving springs mass. *Philos. Trans. A Math. Phys. Eng. Sci.* **382**, 20240037 (2024).
30. Jin, Y., Liu, L., Duan, Z. & Yang, T. Non-smooth nonlocal mechanical diode. *Int. J. Non Linear Mech.* **164**, 104773 (2024).
31. Deshmukh, K. J. Wave-freezing and other phenomena in temporal metasurfaces driven by nonlocal interactions. Preprint at https://arxiv.org/abs2404.09060 (2024).
32. Wang, K., Chen, Y., Kadic, M., Wang, C. & Wegener, M. Nonlocal interaction engineering of 2D roton-like dispersion relations in acoustic and mechanical metamaterials. *Commun. Mater.* **3**, 35 (2022).
33. Zhu, Z. et al. Observation of multiple rotons and multidirectional roton-like dispersion relations in acoustic metamaterials. *New J. Phys.* **24**, 123019 (2022).
34. Moore, D. B., Sambles, J. R., Hibbins, A. P., Starkey, T. A. & Chaplain, G. J. Acoustic surface modes on metasurfaces with embedded next-nearest-neighbor coupling. *Phys. Rev. B* **107**, 144110 (2023).
35. Liu, H. et al. Acoustic topological metamaterials of large winding number. *Phys. Rev. Appl.* **19**, 054028 (2023).
36. Chen, Y., Abouelatta, M. A. A., Wang, K., Kadic, M. & Wegener, M. Nonlocal cable-network metamaterials. *Adv. Mater.* **35**, 2209988 (2023).
37. Sol, J., Röntgen, M. & Del Hougne, P. Covert scattering control in metamaterials with non-locally encoded hidden symmetry. *Adv. Mater.* **36**, 2303891 (2024).
38. Iglesias-Martínez, J. A., Chen, Y. & Wegener, M. Nonlocal conduction in a metawire. *Adv. Mater.* **37**, 2415278 (2025).
39. Bossart, A. & Fleury, R. Extreme spatial dispersion in nonlocally resonant elastic metamaterials. *Phys. Rev. Lett.* **130**, 207201 (2023).
40. Frenzel, T., Kadic, M. & Wegener, M. Three-dimensional mechanical metamaterials with a twist. *Science* **358**, 1072 (2017).
41. Qiu, M. et al. 3D metaphotonic nanostructures with intrinsic chirality. *Adv. Funct. Mater.* **28**, 1803147 (2018).
42. Fernandez-Corbaton, I. et al. New twists of 3D chiral metamaterials. *Adv. Mater.* **31**, e1807742 (2019).
43. Landau, L. Theory of the superfluidity of helium II. *Phys. Rev.* **60**, 356 (1941).
44. Feynman, R. F. & Cohen, M. Energy spectrum of the excitations in liquid helium. *Phys. Rev.* **102**, 1189 (1956).
45. Woods, A. D. B. Neutron inelastic scattering from liquid helium at small momentum transfers. *Phys. Rev. Lett.* **14**, 355 (1965).
46. Godfrin, H. et al. Dispersion relation of Landau elementary excitations and thermodynamic properties of superfluid He 4. *Phys. Rev. B* **103**, 104516 (2021).
47. Mottl, R. et al. Roton-type mode softening in a quantum gas with cavity-mediated long-range interactions. *Science* **336**, 1570 (2012).
48. Godfrin, H. et al. Observation of a roton collective mode in a two-dimensional Fermi liquid. *Nature* **483**, 576 (2012).
49. Chomaz, L. et al. Observation of roton mode population in a dipolar quantum gas. *Nat. Phys.* **14**, 442 (2018).
50. Forcella, D., Prada, C. & Carminati, R. Causality, nonlocality, and negative refraction. *Phys. Rev. Lett.* **118**, 134301 (2017).
51. Wang, K., Chen, Y., Kadic, M., Wang, C. & Wegener, M. Cubic-symmetry acoustic metamaterials with roton-like dispersion relations. *Acta Mech. Sin.* **39**, 723020 (2023).
52. Chen, Y., Li, X., Scheibner, C., Vitelli, V. & Huang, G. Realization of active metamaterials with odd micropolar elasticity. *Nat. Commun.* **12**, 5935 (2021).
53. Farzbod, F. & Scott-Emuakpor, O. E. Interactions beyond nearest neighbors in a periodic structure: force analysis. *Int. J. Solids Struct.* **199**, 203 (2020).
54. Di Paola, M., Failla, G., Pirrotta, A., Sofi, A. & Zingales, M. The mechanically based non-local elasticity: an overview of main results and future challenges. *Philos. Trans. A Math. Phys. Eng. Sci.* **371**, 20120433 (2013).
55. Di Paola, M. & Zingales, M. Long-range cohesive interactions of non-local continuum faced by fractional calculus. *Int. J. Solids Struct.* **45**, 5642 (2008).
56. Yang, L. & Wang, L. Gradient continuum model of nonlocal metamaterials with long-range interactions. *Phys. Scr.* **98**, 15019 (2022).
57. Chen, Y. et al. Phonon transmission through a nonlocal metamaterial slab. *Commun. Phys.* **6**, 1 (2023).
58. Hsu, C. W., Zhen, B., Stone, A. D., Joannopoulos, J. D. & Soljačić, M. Bound states in the continuum. *Nat. Rev. Mater.* **1**, 16048 (2016).
59. Atala, M. et al. Direct measurement of the Zak phase in topological Bloch bands. *Nat. Phys.* **9**, 795 (2013).
60. Hasan, M. Z. & Kane, C. L. Colloquium: topological insulators. *Rev. Mod. Phys.* **82**, 3045 (2010).
61. Rajabpoor Alisepahi, A., Sarkar, S., Sun, K. & Ma, J. Breakdown of conventional winding number calculation in one-dimensional lattices with interactions beyond nearest neighbors. *Commun. Phys.* **6**, 334 (2023).
62. Dal Poggetto, V. F., Pal, R. K., Pugno, N. M. & Miniaci, M. Topological bound modes in phononic lattices with nonlocal interactions. *Int. J. Mech. Sci.* **281**, 109503 (2024).
63. Schindler, F. et al. Higher-order topological insulators. *Sci. Adv.* **4**, t346 (2018).
64. Li, M. et al. Higher-order topological states in photonic kagome crystals with long-range interactions. *Nat. Photon.* **14**, 89 (2020).
65. Sun, Y., Wang, L., Duan, H. & Wang, J. A new class of higher-order topological insulators that localize energy at arbitrary multiple sites. *Sci. Bull.* **70**, 667 (2025).
66. Seppecher, P., Alibert, J. & Isola, F. D. Linear elastic trusses leading to continua with exotic mechanical interactions. *J. Phys.* **319**, 12018 (2011).
67. Dell Isola, F. et al. Pantographic metamaterials: an example of mathematically driven design and of its technological challenges. *Contin. Mech. Thermodyn.* **31**, 851 (2019).
68. Durand, B., Lebée, A., Seppecher, P. & Sab, K. Predictive strain-gradient homogenization of a pantographic material with compliant junctions. *J. Mech. Phys. Solids* **160**, 104773 (2022).
69. Guest, S. D. & Hutchinson, J. W. On the determinacy of repetitive structures. *J. Mech. Phys. Solids* **51**, 383 (2003).
70. Broedersz, C., Mao, X., Lubensky, T. & MacKintosh, F. Criticality and isostaticity in fibre networks. *Nat. Phys.* **12**, 983 (2011).
71. Mao, X. & Lubensky, T. C. Maxwell lattices and topological mechanics. *Annu. Rev. Condens. Matter Phys.* **9**, 413 (2018).
72. Kane, C. L. & Lubensky, T. C. Topological boundary modes in isostatic lattices. *Nat. Phys.* **10**, 39 (2014).
73. Rocklin, D. Z., Chen, B. G., Falk, M., Vitelli, V. & Lubensky, T. C. Mechanical Weyl modes in topological maxwell lattices. *Phys. Rev. Lett.* **116**, 135503 (2016).
74. Abdoul-Anziz, H. & Seppecher, P. Strain gradient and generalized continua obtained by homogenizing frame lattices. *Math. Mech. Complex Syst.* **6**, 213 (2018).
75. Chen, W., Hou, B., Zhang, Z., Pendry, J. B. & Chan, C. T. Metamaterials with index ellipsoids at arbitrary k-points. *Nat. Commun.* **9**, 2086 (2018).
76. Milton, G. W. & Srivastava, A. Further comments on Mark Stockman's article 'Criterion for negative refraction with low optical losses from a fundamental principle of causality'. Preprint at https://arxiv.org/abs/2010.05986 (2020).
77. Lemoult, F., Kaina, N., Fink, M. & Lerosey, G. Wave propagation control at the deep subwavelength scale in metamaterials. *Nat. Phys.* **9**, 55 (2012).
78. Kaina, N., Lemoult, F., Fink, M. & Lerosey, G. Negative refractive index and acoustic superlens from multiple scattering in single negative metamaterials. *Nature* **525**, 77 (2015).
79. Khatibi Moghaddam, M. & Fleury, R. Subwavelength metawaveguide filters and metaports. *Phys. Rev. Appl.* **16**, 044010 (2021).
80. Bossart, A., Dykstra, D. M. J., van der Laan, J. & Coulais, C. Oligomodal metamaterials with multifunctional mechanics. *Proc. Natl Acad. Sci. USA* **118**, e2018610118 (2021).
81. Milton, G. W. & Cherkaev, A. V. Which elasticity tensors are realizable? *J. Eng. Mater. Technol.* **117**, 483 (1995).
82. Kadic, M., Bückmann, T., Stenger, N., Thiel, M. & Wegener, M. On the practicability of pentamode mechanical metamaterials. *Appl. Phys. Lett.* **100**, 191901 (2012).
83. Chen, Y., Liu, X. N. & Hu, G. K. Latticed pentamode acoustic cloak. *Sci. Rep.* **5**, 15745 (2015).
84. Hu, Z. et al. Engineering zero modes in transformable mechanical metamaterials. *Nat. Commun.* **14**, 1266 (2023).
85. Layman, C. N., Naify, C. J., Martin, T. P., Calvo, D. C. & Orris, G. J. Highly anisotropic elements for acoustic pentamode applications. *Phys. Rev. Lett.* **111**, 24302 (2013).
86. Bückmann, T., Thiel, M., Kadic, M., Schittny, R. & Wegener, M. An elasto-mechanical unfeelability cloak made of pentamode metamaterials. *Nat. Commun.* **5**, 4130 (2014).
87. Chen, Y. et al. Broadband solid cloak for underwater acoustics. *Phys. Rev. B* **95**, 180104 (2017).
88. Su, X., Norris, A. N., Cushing, C. W., Haberman, M. R. & Wilson, P. S. Broadband focusing of underwater sound using a transparent pentamode lens. *J. Acoust. Soc. Am.* **141**, 4408 (2017).
89. Chen, Y. & Hu, G. Broadband and high-transmission metasurface for converting underwater cylindrical waves to plane waves. *Phys. Rev. Appl.* **12**, 044046 (2019).
90. Nassar, H., Chen, H. & Huang, G. Microtwist elasticity: a continuum approach to zero modes and topological polarization in kagome lattices. *J. Mech. Phys. Solids* **144**, 104107 (2020).
91. Yu, W., Chen, Y., Liu, X. N. & Hu, G. K. Rayleigh surface waves of extremal elastic materials. *J. Mech. Phys. Solids* **193**, 105842 (2024).
92. Wei, Y. & Hu, G. Wave characteristics of extremal elastic materials. *Extreme Mech. Lett.* **55**, 101789 (2022).
93. Groß, M. F., Schneider, J. L., Chen, Y., Kadic, M. & Wegener, M. Dispersion engineering by hybridizing the back-folded soft mode of monomode elastic metamaterials with stiff acoustic modes. *Adv. Mater.* **36**, 2307553 (2023).
94. Belov, P. A. et al. Strong spatial dispersion in wire media in the very large wavelength limit. *Phys. Rev. B* **67**, 113103 (2003).
95. Shin, J., Shen, J. & Fan, S. Three-dimensional electromagnetic metamaterials that homogenize to uniform non-Maxwellian media. *Phys. Rev. B* **76**, 113101 (2007).
96. Yao, J. et al. Optical negative refraction in bulk metamaterials of nanowires. *Science* **321**, 930 (2008).
97. Simovski, C. R., Belov, P. A., Atrashchenko, A. V. & Kivshar, Y. S. Wire metamaterials: physics and applications. *Adv. Mater.* **24**, 4229 (2012).
98. Ahlfors, L. V. *Complex Analysis* (AMS, 2021).
99. Kohn, W. Analytic properties of Bloch waves and Wannier functions. *Phys. Rev.* **115**, 809 (1959).
100. Romero-García, V., Sánchez-Pérez, J. V. & Garcia-Raffi, L. M. Evanescent modes in sonic crystals: complex dispersion relation and supercell approximation. *J. Appl. Phys.* **108**, 044907 (2010).

101. Chang, Y. & Schulman, J. N. Complex band structures of crystalline solids: an eigenvalue method. *Phys. Rev. B* **25**, 3975 (1982).
102. Laude, V., Achaoui, Y., Benchabane, S. & Khelif, A. Evanescent Bloch waves and the complex band structure of phononic crystals. *Phys. Rev. B* **80**, 92301 (2009).
103. Wang, Y., Wang, Y. & Laude, V. Wave propagation in two-dimensional viscoelastic metamaterials. *Phys. Rev. B* **92**, 104110 (2015).
104. Toupin, R. A. Saint-Venant's principle. *Arch. Ration. Mech. Anal.* **18**, 83 (1965).
105. Camar-Eddine, M. & Seppecher, P. Closure of the set of diffusion functionals with respect to the Mosco-convergence. *Math. Model Methods Appl. Sci.* **12**, 1153 (2002).
106. Camar-Eddine, M. & Seppecher, P. Determination of the closure of the set of elasticity functionals. *Arch. Ration. Mech. Anal.* **170**, 211 (2003).
107. Chen, Y. et al. Observation of floppy flexural modes in a 3D polarized maxwell beam. *Phys. Rev. Lett.* **134**, 86101 (2025).
108. Mindlin, R. D. Micro-structure in linear elasticity. *Arch. Ration. Mech. Anal.* **16**, 51 (1964).
109. Lakes, R. S. & Benedict, R. L. Noncentrosymmetry in micropolar elasticity. *Int. J. Eng. Sci.* **20**, 1161 (1982).
110. Rueger, Z. & Lakes, R. S. Strong cosserat elasticity in a transversely isotropic polymer lattice. *Phys. Rev. Lett.* **120**, 65501 (2018).
111. Duan, S., Wen, W. & Fang, D. A predictive micropolar continuum model for a novel three-dimensional chiral lattice with size effect and tension-twist coupling behavior. *J. Mech. Phys. Solids* **121**, 23 (2018).
112. Frenzel, T. et al. Large characteristic lengths in 3D chiral elastic metamaterials. *Commun. Mater.* **2**, 4 (2021).
113. Liu, X. N., Huang, G. L. & Hu, G. K. Chiral effect in plane isotropic micropolar elasticity and its application to chiral lattices. *J. Mech. Phys. Solids* **60**, 1907 (2012).
114. Chen, Y., Liu, X. N., Hu, G. K., Sun, Q. P. & Zheng, Q. S. Micropolar continuum modelling of bi-dimensional tetrachiral lattices. *Proc. R. Soc. A* **470**, 20130734 (2014).
115. Coulais, C., Kettenis, C. & van Hecke, M. A characteristic lengthscale causes anomalous size effects and boundary programmability in mechanical metamaterials. *Nat. Phys.* **14**, 40 (2017).
116. Kadic, M., Frenzel, T. & Wegener, M. Mechanical metamaterials: when size matters. *Nat. Phys.* **14**, 8 (2018).
117. Pine, A. S. Direct observation of acoustical activity in *n* quartz. *Phys. Rev. B* **2**, 2049 (1970).
118. Kuwata-Gonokami, M. et al. Giant optical activity in quasi-two-dimensional planar nanostructures. *Phys. Rev. Lett.* **95**, 227401 (2005).
119. Gansel, J. K. et al. Gold helix photonic metamaterial as broadband circular polarizer. *Science* **325**, 1513 (2009).
120. Frenzel, T., Köpfler, J., Jung, E., Kadic, M. & Wegener, M. Ultrasound experiments on acoustical activity in chiral mechanical metamaterials. *Nat. Commun.* **10**, 3384 (2019).
121. Chen, Y., Kadic, M., Guenneau, S. & Wegener, M. Isotropic chiral acoustic phonons in 3D quasicrystalline metamaterials. *Phys. Rev. Lett.* **124**, 235502 (2020).
122. Chen, Y., Kadic, M. & Wegener, M. Chiral triclinic metamaterial crystals supporting isotropic acoustical activity and isotropic chiral phonons. *Proc. R. Soc. A* **477**, 20200764 (2021).
123. Chen, Y., Frenzel, T., Zhang, Q., Kadic, M. & Wegener, M. Cubic metamaterial crystal supporting broadband isotropic chiral phonons. *Phys. Rev. Mater.* **5**, 25201 (2021).
124. Portigal, D. L. & Burstein, E. Acoustical activity and other first-order spatial dispersion effects in crystals. *Phys. Rev.* **170**, 673 (1968).
125. Agranovich, V. M. & Ginzburg, V. *Crystal Optics with Spatial Dispersion and Excitons* (Springer, 2013).
126. Chen, Y., Frenzel, T., Guenneau, S., Kadic, M. & Wegener, M. Mapping acoustical activity in 3D chiral mechanical metamaterials onto micropolar continuum elasticity. *J. Mech. Phys. Solids* **137**, 103877 (2020).
127. Muhlestein, M. B., Sieck, C. F., Wilson, P. S. & Haberman, M. R. Experimental evidence of Willis coupling in a one-dimensional effective material element. *Nat. Commun.* **8**, 15625 (2017).
128. Li, Z., Han, P. & Hu, G. Willis dynamic homogenization method for acoustic metamaterials based on multiple scattering theory. *J. Mech. Phys. Solids* **189**, 105692 (2024).
129. Kadic, M., Diatta, A., Frenzel, T., Guenneau, S. & Wegener, M. Static chiral Willis continuum mechanics for three-dimensional chiral mechanical metamaterials. *Phys. Rev. B* **99**, 214101 (2019).
130. Pendry, J. B. A chiral route to negative refraction. *Science* **306**, 1353 (2004).
131. Zhang, S. et al. Negative refractive index in chiral metamaterials. *Phys. Rev. Lett.* **102**, 239012 (2009).
132. Plum, E. et al. Metamaterial with negative index due to chirality. *Phys. Rev. B* **79**, 35407 (2009).
133. Kishine, J., Ovchinnikov, A. S. & Tereshchenko, A. A. Chirality-induced phonon dispersion in a noncentrosymmetric micropolar crystal. *Phys. Rev. Lett.* **125**, 245302 (2020).
134. Chen, Y. et al. Observation of chirality-induced roton-like dispersion in a 3D micropolar elastic metamaterial. *Adv. Funct. Mater.* **34**, 2302699 (2023).
135. Wang, S. et al. Spin–orbit interactions of transverse sound. *Nat. Commun.* **12**, 6125 (2021).
136. Soukoulis, C. M. & Wegener, M. Past achievements and future challenges in the development of three-dimensional photonic metamaterials. *Nat. Photon.* **5**, 523 (2011).
137. Zheludev, N. I. & Kivshar, Y. S. From metamaterials to metadevices. *Nat. Mater.* **11**, 917 (2012).
138. Zangeneh-Nejad, F. & Fleury, R. Active times for acoustic metamaterials. *Rev. Phys.* **4**, 100031 (2019).
139. Nassar, H. et al. Nonreciprocity in acoustic and elastic materials. *Nat. Rev. Mater.* **5**, 667 (2020).
140. Engheta, N. Four-dimensional optics using time-varying metamaterials. *Science* **379**, 1190 (2023).
141. Zhou, Y. et al. Broadband frequency translation through time refraction in an epsilon-near-zero material. *Nat. Commun.* **11**, 2180 (2020).
142. Rizza, C., Castaldi, G. & Galdi, V. Short-pulsed metamaterials. *Phys. Rev. Lett.* **128**, 257402 (2022).
143. Gerken, M. & Miller, D. A. Multilayer thin-film structures with high spatial dispersion. *Appl. Opt.* **42**, 1330 (2003).
144. Moussa, H. et al. Observation of temporal reflection and broadband frequency translation at photonic time interfaces. *Nat. Phys.* **19**, 863 (2023).
145. Jones, T. R., Kildishev, A. V., Segev, M. & Peroulis, D. Time-reflection of microwaves by a fast optically-controlled time-boundary. *Nat. Commun.* **15**, 6786 (2024).
146. Kim, B. L., Chong, C. & Daraio, C. Temporal refraction in an acoustic phononic lattice. *Phys. Rev. Lett.* **133**, 77201 (2024).
147. Liu, Z. et al. Inherent temporal metamaterials with unique time-varying stiffness and damping. *Adv. Sci.* **11**, 2404695 (2024).
148. Kuznetsov, A. I., Miroshnichenko, A. E., Brongersma, M. L., Kivshar, Y. S. & Luk'yanchuk, B. Optically resonant dielectric nanostructures. *Science* **354**, g2472 (2016).
149. Assouar, B. et al. Acoustic metasurfaces. *Nat. Rev. Mater.* **3**, 460 (2018).
150. Chen, W. T., Zhu, A. Y. & Capasso, F. Flat optics with dispersion-engineered metasurfaces. *Nat. Rev. Mater.* **5**, 604 (2020).
151. O'Shea, D. C. *Diffractive Optics: Design, Fabrication, and Test* (SPIE Press, 2004).
152. Yu, N. et al. Light propagation with phase discontinuities: generalized laws of reflection and refraction. *Science* **334**, 333 (2011).
153. Mohammadi Estakhri, N. & Alù, A. Wave-front transformation with gradient metasurfaces. *Phys. Rev. X* **6**, 041008 (2016).
154. Díaz-Rubio, A., Asadchy, V. S., Elsakka, A. & Tretyakov, S. A. From the generalized reflection law to the realization of perfect anomalous reflectors. *Sci. Adv.* **3**, e1602714 (2017).
155. Li, J., Shen, C., Diaz-Rubio, A., Tretyakov, S. A. & Cummer, S. A. Systematic design and experimental demonstration of bianisotropic metasurfaces for scattering-free manipulation of acoustic wavefronts. *Nat. Commun.* **9**, 1342 (2018).
156. Díaz-Rubio, A., Li, J., Shen, C., Cummer, S. A. & Tretyakov, S. A. Power flow-conformal metamirrors for engineering wave reflections. *Sci. Adv.* **5**, u7288 (2019).
157. Zangeneh-Nejad, F., Sounas, D. L., Alù, A. & Fleury, R. Analogue computing with metamaterials. *Nat. Rev. Mater.* **6**, 207 (2021).
158. Xu, G. et al. Arbitrary aperture synthesis with nonlocal leaky-wave metasurface antennas. *Nat. Commun.* **14**, 4380 (2023).
159. Yao, J. et al. Nonlocal metasurface for dark-field edge emission. *Sci. Adv.* **10**, n2752 (2024).
160. Liang, Y., Tsai, D. P. & Kivshar, Y. From local to nonlocal high-Q plasmonic metasurfaces. *Phys. Rev. Lett.* **133**, 53801 (2024).
161. Guo, C., Wang, H. & Fan, S. Squeeze free space with nonlocal flat optics. *Optica* **7**, 1133 (2020).
162. Reshef, O. et al. An optic to replace space and its application towards ultra-thin imaging systems. *Nat. Commun.* **12**, 3512 (2021).
163. Chen, A. & Monticone, F. Dielectric nonlocal metasurfaces for fully solid-state ultrathin optical systems. *ACS Photonics* **8**, 1439 (2021).
164. Momeni, A., Rouhi, K. & Fleury, R. Switchable and simultaneous spatiotemporal analog computing with computational graphene-based multilayers. *Carbon* **186**, 599 (2022).
165. Zhou, Y. et al. Electromagnetic spatiotemporal differentiation meta-devices. *Laser Photon. Rev.* **17**, 2300182 (2023).
166. Esfahani, S., Cotrufo, M. & Alù, A. Tailoring space-time nonlocality for event-based image processing metasurfaces. *Phys. Rev. Lett.* **133**, 63801 (2024).
167. Overvig, A. C., Malek, S. C. & Yu, N. Multifunctional nonlocal metasurfaces. *Phys. Rev. Lett.* **125**, 17402 (2020).
168. Yao, J. et al. Nonlocal meta-lens with Huygens' bound states in the continuum. *Nat. Commun.* **15**, 6543 (2024).
169. Liu, Z. et al. Metasurface-enabled augmented reality display: a review. *Adv. Photonics* **5**, 34001 (2023).
170. Zhu, H., Patnaik, S., Walsh, T. F., Jared, B. H. & Semperlotti, F. Nonlocal elastic metasurfaces: enabling broadband wave control via intentional nonlocality. *Proc. Natl Acad. Sci. USA* **117**, 26099 (2020).
171. Zhou, Z., Huang, S., Li, D., Zhu, J. & Li, Y. Broadband impedance modulation via non-local acoustic metamaterials. *Natl Sci. Rev.* **9**, b171 (2022).
172. Zhou, H. T. et al. Hybrid metasurfaces for perfect transmission and customized manipulation of sound across water–air interface. *Adv. Sci.* **10**, e2207181 (2023).
173. Xie, S. et al. Refined acoustic holography via nonlocal metasurfaces. *Sci. China Phys. Mech. Astron.* **67**, 274311 (2024).
174. Su, G., Du, Z. & Liu, Y. Elastic computational metasurfaces for subwavelength differentiations. *Phys. Rev. B* **109**, L161108 (2024).
175. Zeng, H. et al. Nonlocal acoustic–mechanical metasurface for simultaneous and enhanced sound absorption and vibration reduction. *Mater. Des.* **244**, 113120 (2024).
176. Li, X. et al. Ultrathin acoustic holography. *Adv. Mater. Interfaces* **10**, 2300034 (2023).
177. Han, C. et al. Nonlocal acoustic moire hyperbolic metasurfaces. *Adv. Mater.* **36**, e2311350 (2024).
178. Toll, J. S. Causality and the dispersion relation: logical foundations. *Phys. Rev.* **104**, 1760 (1956).
179. Wang, Y., Jen, H. H. & You, J. Scaling laws for non-Hermitian skin effect with long-range couplings. *Phys. Rev. B* **108**, 85418 (2023).
180. Miller, D. A. Why optics needs thickness. *Science* **379**, 41 (2023).

181. Li, Y. & Monticone, F. Exploring the role of metamaterials in achieving advantage in optical computing. *Nat. Comput. Sci.* **4**, 545 (2024).
182. Li, Y. & Monticone, F. The spatial complexity of optical computing and how to reduce it. Preprint at https://arxiv.org/abs/2411.10435 (2024).
183. Fu, T. et al. Optical neural networks: progress and challenges. *Light Sci. Appl.* **13**, 263 (2024).

Acknowledgements
The authors acknowledge financial support by the Deutsche Forschungsgemeinschaft (German Research Foundation) under Germany's Excellence Strategy via the Excellence Cluster '3D Matter Made to Order', EXC-2082/1-390761711, by the Carl Zeiss Foundation through the 'Carl-Zeiss-Foundation-Focus@HEiKA', by the State of Baden-Württemberg and by the Helmholtz programme 'Materials Systems Engineering'. R.F. acknowledges the support of the Swiss National Science Foundation under the Eccellenza award PCEGP2_181232 for the research project titled 'Ultra-compact wave devices based on deep sub wavelength spatially dispersive effects'. G.H. thanks the support of National Natural Science Foundation of China (Grant No. 11991030).

Author contributions
Y.C. and M.W. drafted the initial version. All authors contributed to the discussions and the revision of this paper.

Competing interests
The authors declare no competing interests.

Additional information
Peer review information *Nature Reviews Physics* thanks Kshiteej Deshmukh, Francesco Monticone and Shuang Zhang for their contribution to the peer review of this work.